Electronic Supplementary Material (ESI)

Incorporating Redox Active Entity to Attain Electrical Bistability in a Polymer Semiconductor

Biswajit K. Barman,[a†] Nani G. Ghosh,[a†] Indrajit Giri,[a] Chandan Kumar,[a] Sanjio S. Zade,*[a] Ratheesh K. Vijayaraghavan*[a]

a. Department of Chemical Sciences and Center for Advanced Functional Materials, Indian Institute of Science Education and Research Kolkata, Mohanpur, Nadia, West Bengal-741246.

† Equal contribution

Email: ratheesh@iiserkol.ac.in

Table of Contents

1. Materials and Methods:

The moisture sensitive substrate involving reactions were performed using well dried two necked RB. The products are stored in a capped vial in some well dry places. Reactions were monitored on TLC using Merck silica gel 60 F-254 thin-layer plates under UV lamp (254 nm). Column chromatography was done on Silica Gel (100-200 mesh).

Synthesis:

All the reactions were done under nitrogen environment to maintain dry conditions. Before use, toluene and THF (tetrahydrofuran) were distilled from sodium/benzophenone. 1,5-dihydroxyanthraquinone(anthrarufin), Thiophene, $Pd(PPh_3)_4$, Tris(dibenzylideneacetone)dipalladium(0)-chloroform adduct $\{Pd_2(dba)_3{\cdot}CHCl_3\}$, 2-Thiophenecarbonitrile, Tris(o-tolyl)phosphine $P(o\text{-tol})_3$, and $TBAPF_6$ were acquired from Aldrich and used without further purification. Iodine and iodic acid were purchased from Merck and Aldrich, respectively, and were used without further purification. *n*-BuLi (1.6 M in hexane) was purchased from Spectrochem.

2. Measurement and characterization:

^1H NMR and ^{13}C NMR spectra of the compounds were recorded using a JEOL ECS 400 MHz and BRUCKER AVANCE 500 MHz spectrometer with $CDCl_3$ or DMSO-d_6 as the solvent, and chemical shifts (δ) are reported in parts per million (ppm) relative to tetramethylsilane as the internal standard values. The coupling constants (J) are given in Hz. The apparent resonance multiplicity is described as s (singlet), br s (broad singlet), d (doublet), t (triplet), q (quartet), and m (multiplet). High-Resolution Mass spectroscopy (HRMS) data has been recorded in LC/ESI/HRMS (Bruker, MAXIS/IMPACT) using MeOH or ACN. The UV-Vis spectra were recorded on model Perkin Elemer Lamba 35 UV-VIS spectrometer and Fluorescence spectra recorded on Horiba JobinYvon, Fluoromax-3 (Xe-150 W, 250-900 nm). The cyclic voltammogram measurement: Cyclic Voltammetry was recorded with CHI604D instrument. Cyclic Voltammetry for liquid state samples was determined at room temperature using 0.1 M Bu_4NPF_6 solutions as the electrolyte in dry acetonitrile solvent under argon atmosphere with a scan rate of 100 mV/s using a three-electrode configuration {Gold as working electrode, Pt wire as the counter electrode, Ag/AgCl (saturated KCl) as the reference electrode}. Semi contact mode AFM (atomic force microscopy) experiments were performed using Nova NT-MDT instrument

(Model No. AP-0100). Resonance frequency used for the experiment was 271.12 KHz with a scan rate of 0.6 Hz and the lateral resolution used for the AFM experiment was 3.9 nm and vertical resolution used nearly 0.1 nm.

3. Synthetic procedure:

3,6-di(thiophen-2-yl)-2,5-dihydropyrrolo[3,4-c]pyrrole-1,4-dione[1], 2,5-bis(2-ethylhexyl)-3,6-di(thiophen-2-yl)-2,5-dihydropyrrolo[3,4-c]pyrrole-1,4-dione[1], 1,5-bis((2-ethylhexyl)oxy)-4,8-diiodoanthracene-9,10-dione[2] were synthesized according to the previously reported procedure.

1,5-bis((2-ethylhexyl)oxy)-4 ,8-bis(tributylstannyl)anthracene-9,10-dione (1).

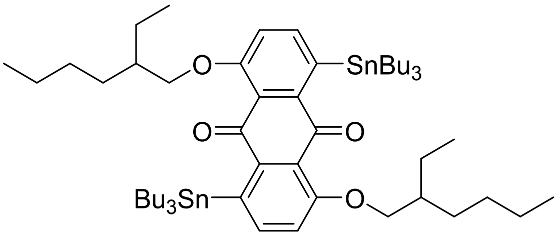

A solution of 1,5-bis((2-ethylhexyl)oxy)-4,8-diiodoanthracene-9,10-dione (500 mg, 0.7 mmol), 1,1,1,2,2,2-hexabutyldistannane (405 mg, 0.7 mmol), and tri(*o*-tolyl)phosphine (107 mg, 0.35 mmol) in dry toluene (15 ml) was deoxygenated with nitrogen for 5 min. $Pd_2(dba)_3$ (64 mg, 0.07 mmol) was added and the reaction was heated to 90 °C for 18 h. After cooling, the solvent was removed under reduced pressure. The crude product was purified by flash column chromatography in basified alumina to yield a yellow viscous oil (410 mg, 56%).

^{1}H NMR (400 MHz, $CDCl_3$): δ 7.89 (2 H, d, *J* 8.3), 7.26 (2 H, d, *J* 8.2), 4.04 (4 H, m), 1.81 (2 H, m), 1.56 (14 H, m), 1.36 (24 H, m), 1.13 (10 H, m), 1.01 (8 H, m), 0.96 (6 H, m), 0.90 (20 H, m).

^{13}C NMR (126 MHz, $CDCl_3$): δ 184.45, 160.53, 143.40, 141.84, 135.78, 121.93, 116.69, 71.41, 40.00, 30.62, 29.57, 27.76, 23.96, 23.33, 14.38, 13.99, 11.65, 11.41, 9.00.

HRMS: (ESI) Calculated for $C_{54}H_{92}O_4Sn_2$ $[M]^+$: 1042.50, found 1042.45.

3,6-bis(5-bromothiophen-2-yl)-2,5-bis(2-ethylhexyl)-2,5-dihydropyrrolo[3,4-c]pyrrole-1,4-dione (2).

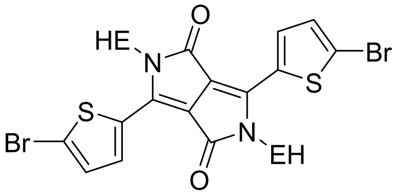

3,6-Di(thiophen-2-yl)-2,5-dihydropyrrolo[3,4-c]pyrrole-1,4-dione (525 mg, 1 mmol) was dissolved in distilled chloroform (15 ml) and then NBS (338 mg, 1.9 mmol) was added to it in the absence of light in portions at rt. After stirring overnight at rt, water was added to the reaction mixture. The reaction mixture was extracted with 3×20 ml chloroform and then purified by silica gel column chromatography with DCM/hexane 10-20% to obtain compound **2** as bluish-purple solid and ^{1}H NMR matches with the previously reported procedure.[1]

^{1}H NMR: (400MHz, $CDCl_3$): δ 8.63 (2 H, d, *J* 4.2), 7.22 (2 H, d, *J* 4.2), 3.93 (4 H, s), 1.83 (2 H, m), 1.38-1.25 (16 H, s), 0.89 (12 H, s).

Synthesis of polymer (AQ2TDPP):

The polymer was prepared from a palladium-catalyzed Stille coupling reaction. To a two-neck flask, 1,5-bis((2-ethylhexyl)oxy)-4,8-bis(tributylstannyl)anthracene-9,10-dione (**1**) (375 mg, 0.3 mmol), 3,6-bis(5-bromothiophen-2-yl)-2,5-bis(2-ethylhexyl)-2,5-dihydropyrrolo[3,4-c]pyrrole-1,4-dione (**2**), (205 mg, 0.3 mmol), and chlorobenzene (5 ml) were added under nitrogen. The mixture was stirred for 30 min, and then $Pd_2(dba)_3{\cdot}CHCl_3$ (31 mg, 0.03 mmol) and $P(o\text{-tol})_3$ (46 mg, 0.15 mmol) was added. The mixture was heated up to 130 ^{o}C and stirred for 72 h. After the reaction was finished, the mixture was cooled to room temperature and poured into methanol. The precipitated solid was filtered and carried out further purification via Soxhlet extraction (methanol, acetone, and chloroform) successively. After the extraction was completed, the chloroform solution was concentrated and poured into the methanol. The precipitated solid was filtered and dried. Yield: 165 mg (62$^{\%}$).

^{1}H NMR (400 MHz, $CDCl_3$): δ 8.98 (2H, br), 7.66 (2H, br), 7.20 (2H, br), 4.09 (8H, br), 2.05 (2H, br), 1.45 (8H, br), 1.34 (10H, br), 1.29 (6H, br), 1.26 (8H, br), 0.91 (24H, br).

Table S1. Physical properties of **AQ2TDPP**.

	M_n (kDa)	M_w (kDa)	D	T_d (°C)
AQ2TDPP	9.4	11.18	1.18	218

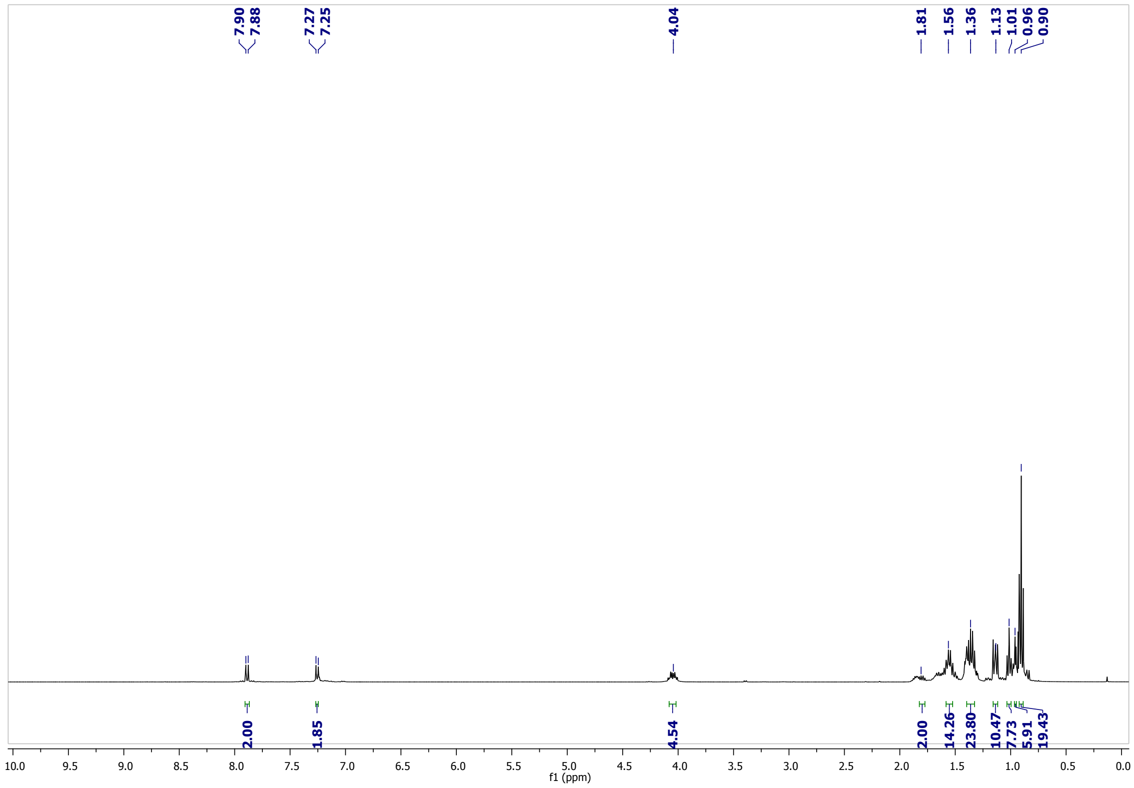

Figure S1: ^{1}H NMR spectra of compound **1.**

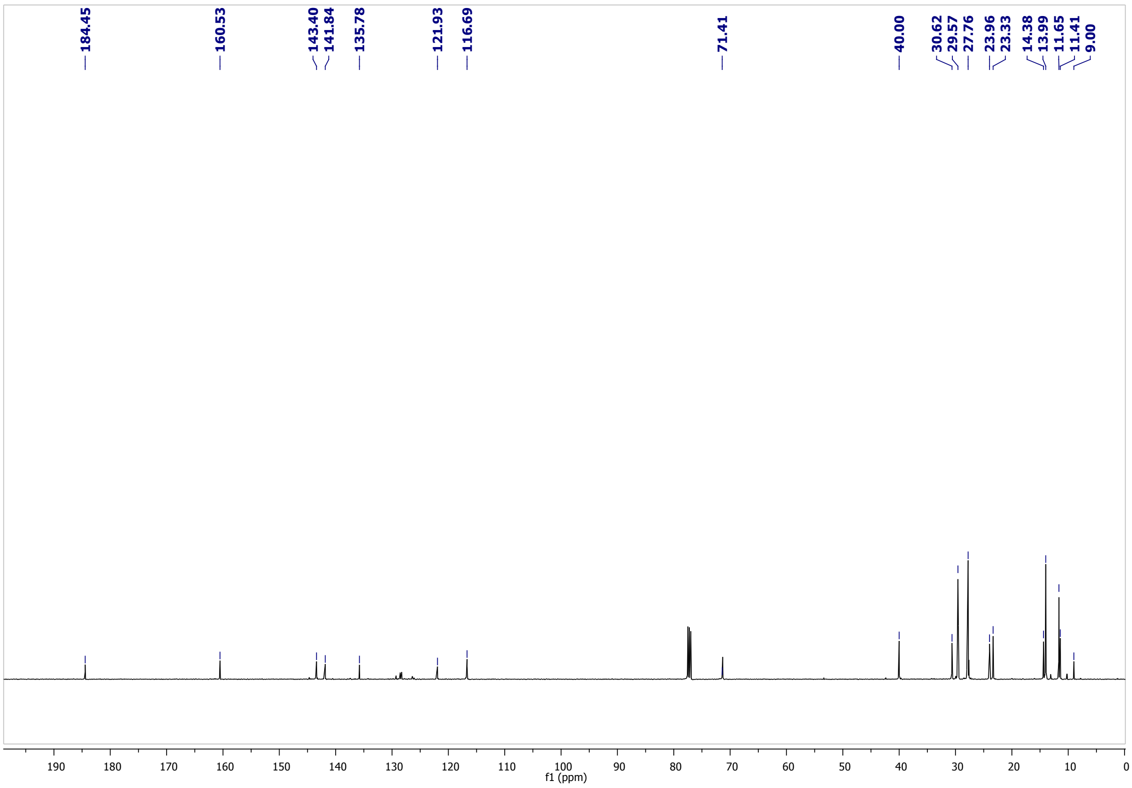

Figure S2: ^{13}C NMR spectra of compound **1.**

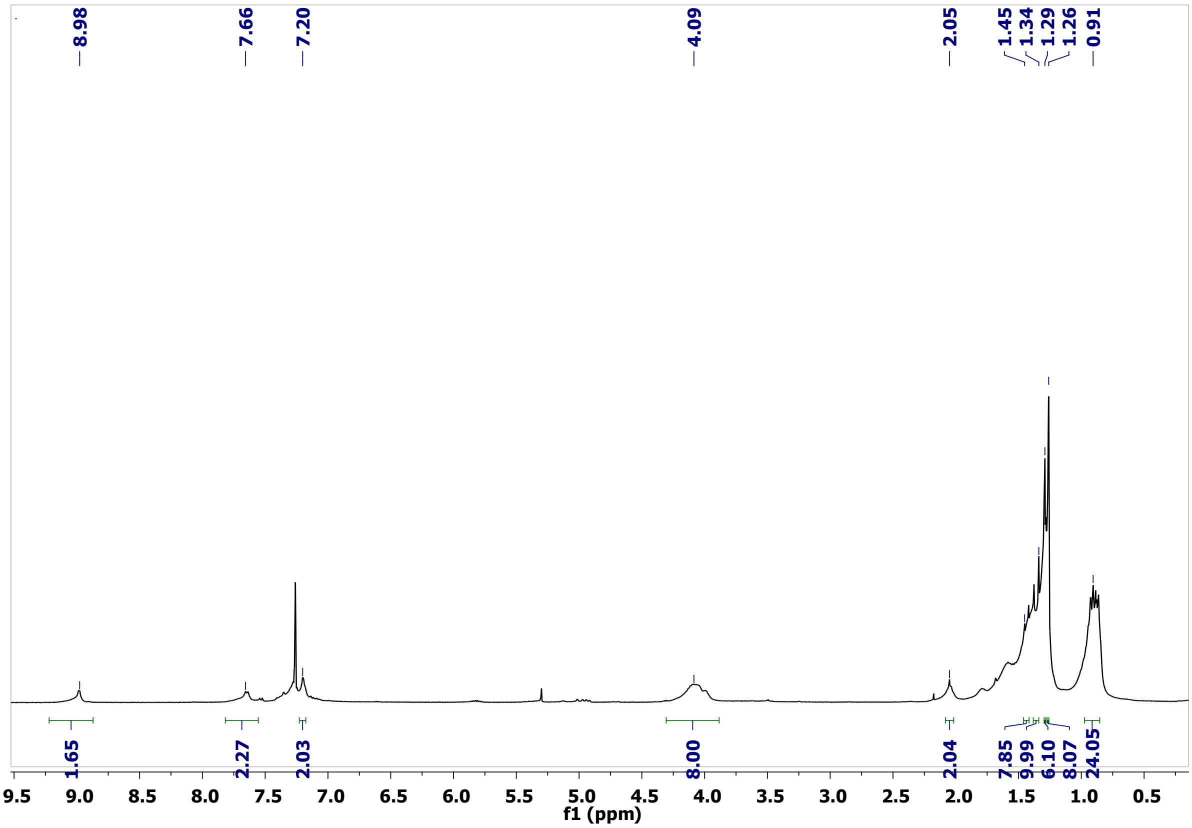

Figure S3: ^{1}H NMR spectra of **AQ2TDPP.**

4. Thermal stability of AQ2TDPP.

Thermal stability is one of the essential properties that a polymer should possess for its practical application as an electronic material. Thermal stability was tested for the polymers by thermogravimetric analysis (TGA) at a heating rate of 10 °C min^{-1} under nitrogen gas flow. The decomposition temperature (T_d) is defined as the temperature at which a polymer loses 5% of its initial mass. **AQ2TDPP** exhibit good thermal stability with a T_d value of 218 °C (Figure S4).

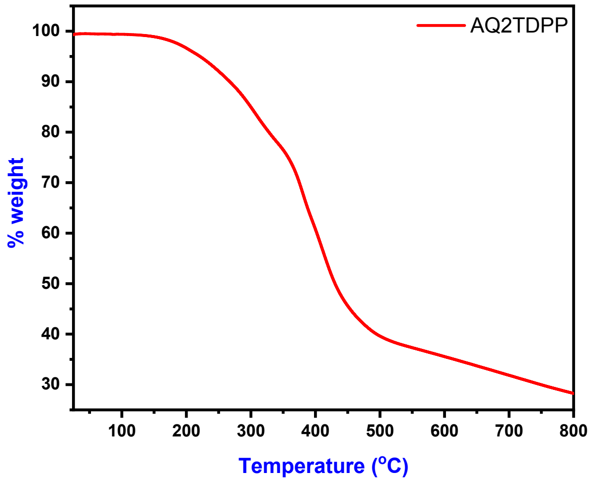

Figure S4: TGA thermogram of **AQ2TDPP** at a heating rate of 10 °C/min.

5. Optical and electrochemical properties:

UV-Vis spectroscopic measurements were carried out in Agilent Technologies Cary 8454 spectrophotometer. The cyclic voltammogram measurement: Cyclic Voltammetry was recorded with CHI604D instrument. Cyclic Voltammetry for liquid state samples was determined at room temperature using 0.1 M Bu_4NPF_6 solutions as the electrolyte in dry acetonitrile solvent under argon atmosphere with a scan rate of 100 mV/s using a three-electrode configuration {Gold as working electrode, Pt wire as the counter electrode, Ag/AgCl (saturated KCl) as the reference electrode}. HOMO and LUMO energy levels of compound were calculated according to the inner reference ferrocene redox couple versus Ag/Ag^+ in acetonitrile by using the following formula,

$$E_{LUMO} = -[E_{red}^{onset} + 4.8 - E_{Fc/Fc+}^{1/2}]$$

	E_{red} ^{onset} (V)	E_{LUMO} (eV)	ΔE_g^{opt} (eV)	E_{HOMO} (eV)	HIB (eV)	EIB (eV)
AQ2TDPP	-0.71	-3.61	1.85	-5.46	0.66	0.49

Table S2: Redox potentials of the polymer, where E_{red}^{onset} is the first reduction potential, E_{LUMO} is the LUMO energy, E_{HOMO} is the HOMO energy, ΔE_g^{opt} is the optical band gap which is determinate from equation 1240/λ (nm), HIB is the hole injection barrier, and the EIB is the electron injection barrier w.r.to the work function of the injection contacts.

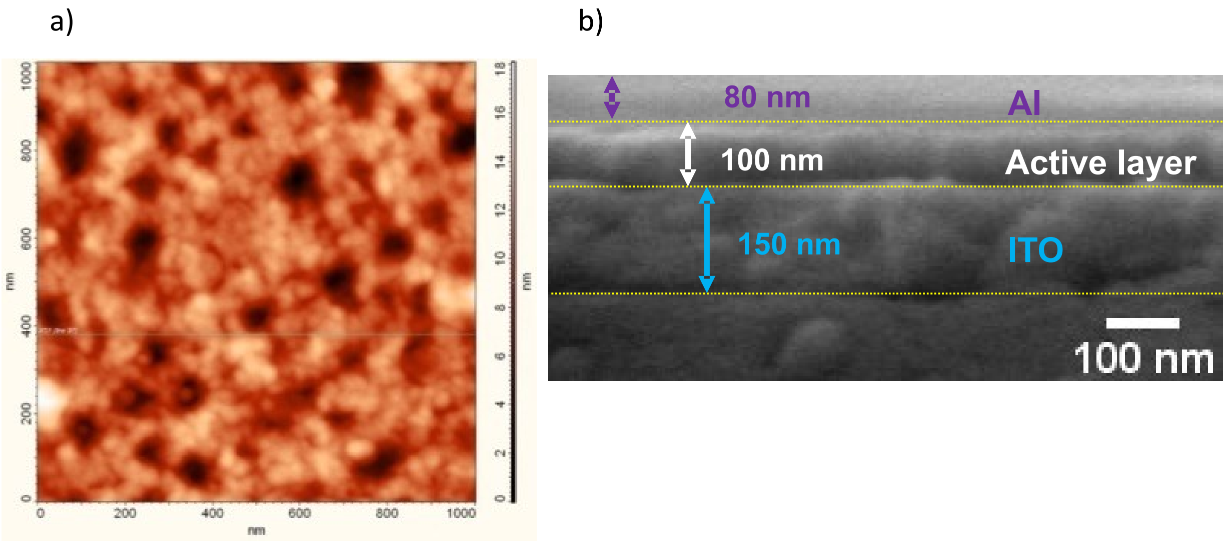

Figure S5: a) AFM image of the **AQ2TDPP** film on top of ITO surface and b) cross-sectional SEM image of the resistive memory device.

6. DFT calculations:

All calculations were performed by density functional theory (DFT) method using Gaussian 16 program package. The geometry of the monomer unit was optimized by means of B3LYP (Becke three parameters hybrid functional with Lee–Yang–Parr correlation functional) level of theory. The 6-31g (d,p) basis set was used for all atoms (C, H, O, S and N) present in the monomer. Time-dependent density functional theory (TDDFT) of the ligand was performed using the same basis set, B3LYP/6-31G(d,p) for determining vertical electronic transitions. The molecular orbitals were visualized using the Avogadro molecular editor. Oscillator strength value obtained from TD DFT calculation using GaussView 6.0.16.

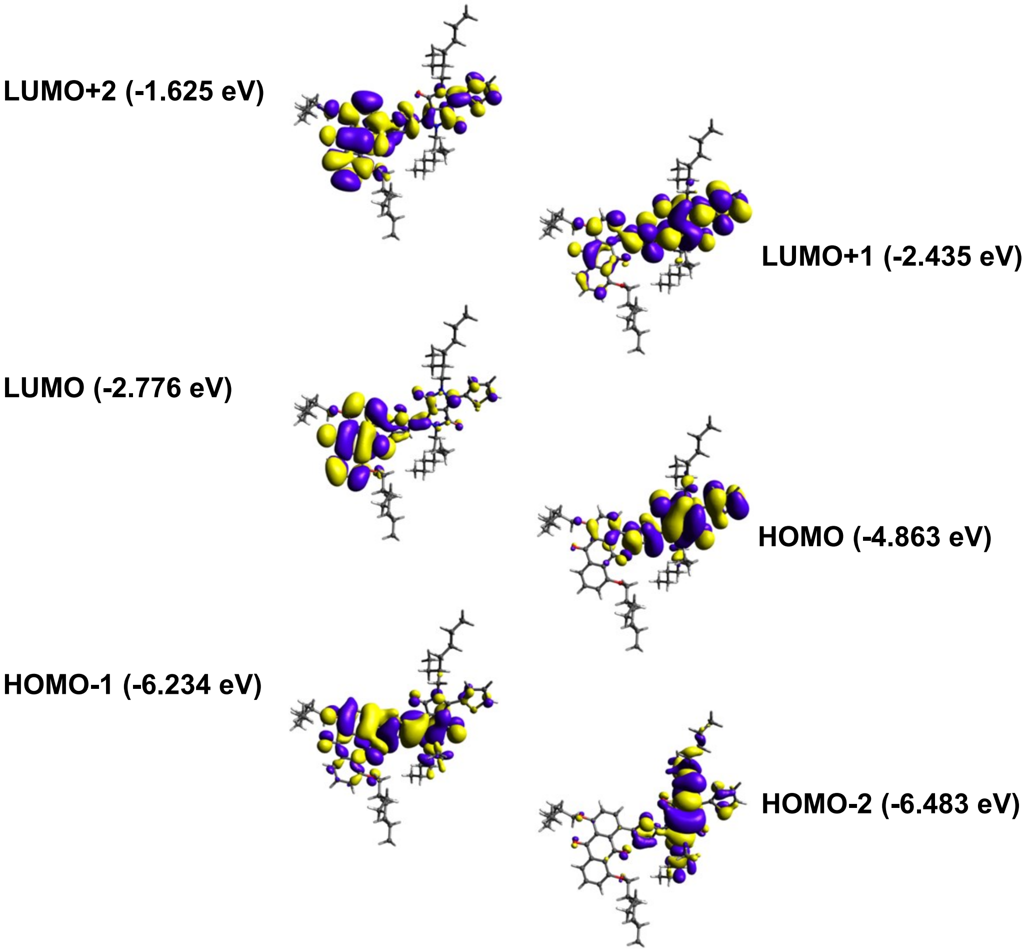

Figure S6: Frontier molecular orbital (FMO) plots and energy levels of designed polymer repeating unit at the B3LYP/6-31G (d,p) level of theory. Isovalue used for calculation is 0.01.

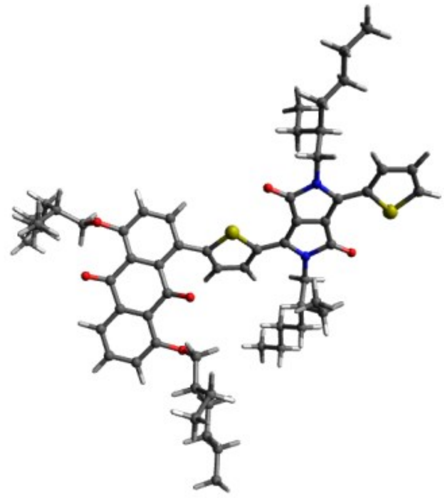

Figure S7: Molecular optimised geometry of the repetive unit of **AQ2TDPP**.

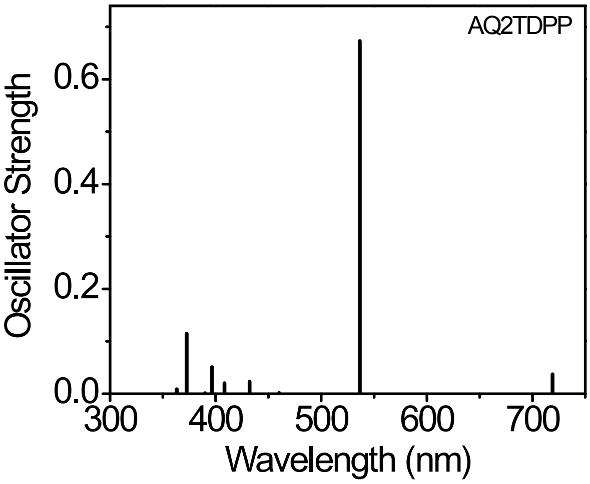

Figure S8: TD-DFT calculated oscillator strength vs wavelength plot of polymer repeating unit at the B3LYP/6-31G (d,p) level of theory.

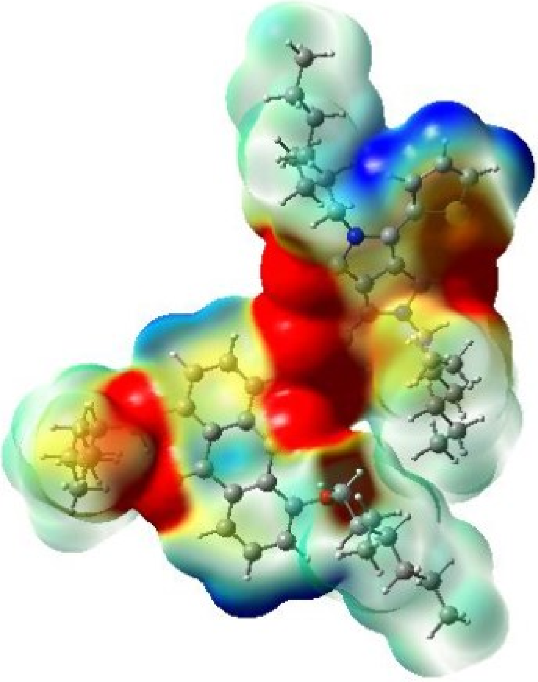

Figure S9: Electronic surface potentials (ESP) of polymer repeating unit at the B3LYP/6-31G (d,p) level of theory. Isovalue used for calculation is 0.0004.

7. Device fabrication:

Memory devices were fabricated on indium tin oxide (ITO) coated glass substrates, which were cleaned by soap water; 2-isopropanol and acetone accordingly and finally keep it for 30 minutes in UV ozone cleaner. Solid powders of polymer (**AQ2TDPP**) was first dissolved in chloroform (10 mg /1.0 ml). This solution was spin-coated on ITO coated substrates at 2000 rpm for 40 seconds to yield nearly 100 nm thick films of the active layer. Top electrode aluminium (Al) was vacuum evaporated on top of the films from a tungsten filament basket at a pressure below 4.2 x 10^{-6} mbar. We fabricated hole only device (HOD) with a structure based on ITO/poly(3,4-ethylenedioxythiophene)-poly(styrenesulfonate)(PEDOT:PSS)/**AQ2TDPP**/Gold(Au) and extracted the hole mobilities of polymer from the space charge limited current (SCLC) regime of J−V curves based on the Mott−Gurney law, $J = (9/8)\varepsilon_0\varepsilon_r\mu V^2/d^3$ where J is the current density, ε_0 is the vacuum permittivity, ε_r is the relative dielectric constant of the organic semiconductor (here, we used 3), μ is the hole mobility, V is the applied voltage, and d is the thickness of the HTM which was estimated to be around 100 nm. We fabricated electron only device (EOD) with a structure based on indium tin oxide (ITO)/ZnO/**AQ2TDPP**/Al and extracted the electron mobilities of polymer in a similar way like hole only device. In HOD, PEDOT-PSS coated at 4510 rpm for 20s on top of ITO. For EOD, ZnO coated at 2000 rpm for 60s on top of ITO and top electrode Au was vacuum evaporated on top of the films from a tungsten filament basket at a pressure below 3.2 x 10^{-6} mbar. I-V characteristics were measured by KEITHLEY (2450 Source Meter). All the measurements were carried out at room temperature under an ambient atmosphere in the absence of light.

Device type	Device layer structure	Active layer thickness
Resistive memory	ITO/Polymer/Al	100 nm
Electron only device	ITO/ZnO/Polymer/Al	100 nm
Hole only device	ITO/PEDOT-PSS/Polymer/Au	100 nm

Table S3. Summarized device structures.

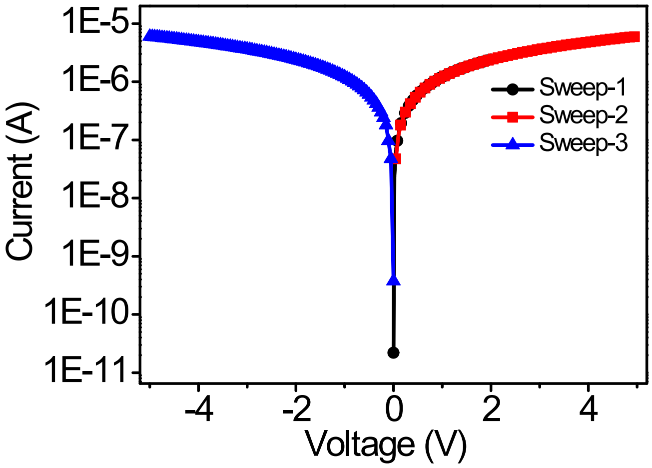

Figure S10: Characteristic I-V responses of **2TDPP**.

Device geometry	V_{SET}/ V_{RESET} (V)	Retention time (s)	Mechanism	Ref
Al/TP6F-PI/ITO	3.2 /-2.1	>11,000	CT complex formation.	3
ITO/P-(BPPO)-PI/Al	2.3 /-2.5	18,000	Electric field-induced CT	4
ITO/OAQ-6FPI/Al	-3.9	10,000	Intermolecular /intra molecular CT	5
PEN/Al/polymer/Al	-2.5 (PVC-PI)	10,000	The charge trapping/detrapping mediated CT process	6
ITO/polymer/Al	-3.7	3600	Intermolecular /intra molecular CT	7
ITO/ Active layer /Al	-1.6 / 2.8	>7,000	CT State formation	8
ITO/ 6F-CzTZ PI/ Au	1.6	4,000	Electric- field- induced CT	9
ITO/Polymer /Al	-3.3	3600	CT mechanism	10
ITO/Polymer /Au	2.2 / 2.6 (2.7)	4000 600	CT complex/	11
ITO/ Compound (Small molecule)/ Al	-2.2 ,-3.09 / 2.97	10,000	CT complex - field-induced charge transfer (CT)	12
ITO/PU(IPDI-AQ-EG)/Al	-2.7 /2.8	3000	Conductive CT complex	13
Al/PI-a/ITO Al/PI-b/ITO	-0.2 to -0.4 -2.6 & -2.4	2000 2000	CT processes	14
ITO/PFTPA-Fc/Pt	-	10,000	The oxidation of ferroene and triphenylamine groups.	15
ITO/Polymer /Al	2.5 / -1.8	30,000	CT mechanism	This work

Table S4: Summary of the comparative device switching mechanisms known in literature.

8. References:

1 E. Heyer and R. Ziessel, *Synlett*, 2015, **26**, 2109-2116.

2 N. G. Ghosh, A. Sarkar and S. S. Zade, *Chem. Eng. J*, 2020, **407**, 127227.

3 Q. D. Ling, F. C. Chang, Y. Song, C. X. Zhu, D. J. Liaw, D. S. H. Chan, E. T. Kang and K. G. Neoh, *J. Am. Chem. Soc.*, 2006, **128**, 8732–8733.

4 Y. L. Liu, K. L. Wang, G. S. Huang, C. X. Zhu, E. S. Tok, K. G. Neoh and E. T. Kang, *Chem. Mater.*, 2009, **21**, 3391–3399.

5 Y. C. Hu, C. J. Chen, H. J. Yen, K. Y. Lin, J. M. Yeh, W. C. Chen and G. S. Liou, *J. Mater. Chem.*, 2012, **22**, 20394–20402.

6 C. J. Chen, H. J. Yen, Y. C. Hu and G. S. Liou, *J. Mater. Chem. C*, 2013, **1**, 7623–7634.

7 H. C. Wu, C. L. Liu and W. C. Chen, *Polym. Chem.*, 2013, **4**, 5261–5269.

8 W. P. Lin, S. J. Liu, T. Gong, Q. Zhao and W. Huang, *Adv. Mater.*, 2014, **26**, 570–606.

9 L. Shi, N. Jia, L. Kong, S. Qi and D. Wu, *Macromol. Chem. Phys.*, 2014, **215**, 2374–2388.

10 J. H. Wu and G. S. Liou, *ACS Appl. Mater. Interfaces*, 2015, **7**, 15988–15994.

11 N. Jia, S. Qi, G. Tian, X. Wang and D. Wu, *J. Electron. Mater.*, 2017, **46**, 2011–2020.

12 Q. Zhang, J. He, H. Li, N. Li, Q. Xu, D. Chen and J. Lu, *J. Mater. Chem. C*, 2017, **5**, 7961–7968.

13 Y. Yang, H. Lu, J. Liu and Y. Shen, *Eur. Polym. J.*, 2018, **108**, 10–19.

14 Y. Li, M. Zhou, Z. Yang and Y. Li, *J. Mater. Sci.*, 2018, **53**, 15600–15613.

15 B. Zhang, F. Fan, W. Xue, G. Liu, Y. Fu, X. Zhuang, X. H. Xu, J. Gu, R. W. Li and Y. Chen, *Nat. Commun.*, 2019, **10**, 736.